

Role of Activated Protein C and Soya-bean in Experimental Lung Toxicity in Adult Male Albino Rat: Histological and Immunohistochemical Studies

Maha Mohamed Abo Gazia¹ and Eman Ali Mahmoud El-Kordy²

¹Histology Department, Faculty of Medicine, Al-Fayoum University

²Histology Department, Faculty of Medicine, Tanta University

mahaabogazia@yahoo.com

Abstract: Background: Amiodarone (AM) is a potent antiarrhythmic drug that is limited in clinical use by its adverse effects, including potentially life-threatening AM-induced pneumotoxicity. The resemblance of the morphologic changes in amiodarone-treated rats lungs to pulmonary toxicity in humans suggest that this form of chemical injury may serve as useful model of this disease entity. **Aim of the Work:** Studying the effect of amiodarone on the lung of rat histologically and immunohistochemically as well as the role of concomitant use of soybean and activated protein C (APC) in ameliorating pulmonary toxicity (pneumotoxicity or parenchymal lung disease) induced by amiodarone. **Material and Methods:** Thirty adult male albino rats were used for the present study. The animals were divided into four groups: group I (control), group II (each rat was amiodarone orally treated for 6 weeks), group III (each animal was given soybean and amiodarone for 6 weeks) and group IV (each animal was given activated protein C and amiodarone for 6 weeks). The lung was then examined histologically and immunohistochemically. **Results:** Amiodarone caused increased interalveolar thickness with increased cellularity and mononuclear cellular infiltrations. Hypercellularity involved macrophages with large vacuolated cytoplasm and hyperplastic type II pneumocytes in group II. There was congested blood capillaries with some extravastion of red blood cells. By electron microscope, the hypertrophied type II pneumocytes showed multiple lamellar bodies and small inclusions with dilated rough endoplasmic reticulum. Macrophages with eccentric nuclei and prominent lamellar bodies with increased lysosomes were detected in group II. Also, increasing collagen fibers were detected. Rats treated with APC and soybean showed attenuation of these changes. There was a significant increase in plasminogen activator inhibitor-1 (PAI-1) immunoreaction in group II with nonsignificant change in group III and group IV.

[Maha Mohamed Abo Gazia and Eman Ali Mahmoud El-Kordy. **Role of Activated Protein C and Soya-bean in Experimental Lung Toxicity in Adult Male Albino Rat: Histological and Immunohistochemical Studies.** Life Science Journal 2012; 9(2):73-85]. (ISSN: 1097-8135). <http://www.lifesciencesite.com>. 14

Key Words: Activated Protein C, Soya-bean, Lung Toxicity, plasminogen activator inhibitor-1 (PAI-1), lamellar bodies.

1. Introduction:

Pulmonary toxicity is a complex, chronic illness that may result from a variety of acute and chronic lung diseases (*Martin and Rosenow, 1988*). The excessive accumulation of matrix proteins, mainly produced by fibroblasts and myofibroblasts, is responsible for impairment in alveolar walls, loss of elasticity and development of rigid lung (*Massey et al., 1995*). The progression of pulmonary fibrosis is closely related to a complicated network consisting of many chemical mediators, coagulation abnormalities and endothelial cells (*Blake and Reasor, 1995*). Procoagulant signalling mechanisms as a member of this network, contributes to the development of lung inflammation and fibrosis in acute lung injury and fibrotic lung disease (*Idell, 2003*).

Amiodarone is a potent antiarrhythmic drug whose use has been limited due to numerous side effects (*Waerhaug et al., 2009*). One of the more serious side effects is the development of pulmonary toxicity (*Massey et al., 1995*). As the use of amiodarone increases, the occurrence of its side

effects will likely increase accordingly. Despite a great deal of information regarding the mechanisms of amiodarone-induced lung injury, management of this lung disorder is frequently difficult, and unfortunately therapeutic approaches to inhibit the development of amiodarone pulmonary toxicity are scanty (*Padmavathy et al., 1992*).

Emerging evidence that amiodarone administration results in interstitial alveolar inflammation and reports from earlier studies mentioned that coagulation abnormalities with oxidative metabolic reactions in lung injury are compelling reasons to use APC and soybean in suppressing amiodarone induced pulmonary toxicity (*Padmavathy et al., 1992*).

Several studies suggest that oxidant-antioxidant imbalances in the lower respiratory tract play a critical role in the pathogenesis of pulmonary injury. For example, pulmonary inflammatory cells of patients with pulmonary injury generate higher levels of oxidants than those in control patients (*Padmavathy et al., 1992*).

Soybean has been a food in china for thousands of years. It is an abundant, economic source of protein. No other nation has acquired the same taste for soybean as the Chinese and Japanese, but the bean has become an important raw material for the international food industry (*Liechtenstein, 1998*). Attention has recently focused on the possible role of soybean in the diet for the prevention and treatment of degenerative diseases (*Messina, 1999*). Several studies documented the hypocholesterolaemic, anticarcinogenic effects of soybean as well as its role in lowering the risk of osteoporosis (*Ishimi et al., 1999*).

The health benefits of soybean and its products have been documented (*Mitchell et al., 1998*). The active components of the soybean products responsible for these effects have yet to be defined. It is believed that isoflavones, genistein and daidzein are responsible for these observed benefits (*Malencic et al., 2007*). Soy-bean isoflavones may play a beneficial role in preventing hormone-related disorders such as breast cancer and autoimmune diseases. Soybean isoflavones, exhibited in vitro, strong antioxidant potency in decreasing the risk of coronary heart disease, osteoporosis and chronic renal disease (*Mahwah, 1996*). Several studies have shown that supplementations with either purified isoflavones (genistein and daidzein) or 80% methanol extract (containing isoflavones) from several soy food including tofu, inhibited reactive nitrogen species-induced oxidation that cause many chronic diseases such as interstitial lung disease (*Silva et al., 2002*). Soybean polyphenol content may act also as antioxidant, thereby reducing the risk of pulmonary injury and atherosclerosis (*Su et al., 2000*). As most of the previous studies reported the effect of soybean on lung injury biochemically, the current study evaluated the role of soybean on lung-induced toxicity histologically and immunohistochemically.

There is increasing evidence that the activation of the coagulation cascade with the resultant extravasation of active coagulation proteinases into alveolar tissue may play an important role in the pathogenesis of lung toxicity (*Chambers, 2008*).

The protein C (PC) pathway is one of the most important regulators of the blood coagulation system (*Dhainaut et al., 2004*). The zymogen PC is converted into its active form, activated PC (APC) via thrombomodulin-thrombin complex on the phospholipid surface of endothelial cells, monocytes and platelets (*Jian et al., 2005*). Recent studies have demonstrated that, in addition to its regulatory function on the coagulation system, APC may also regulate the inflammatory responses (*Looney et al., 2009*). APC is decreased in many pathological states, e.g. endotoxin induced pulmonary vascular injury and

Escherichia coli in experimental animal models of sepsis (*Richard et al., 2007*). Therefore, we hypothesized that APC may improve lung histology and function in an animal model of lung induced toxicity using light and electron microscopy.

2. Material and Methods:

Chemicals:

Amiodarone: hydrochloride-aniodinated benzofuran derivative was obtained from Sanofi Pharmaceuticals Company, France. Each 1 mg was dissolved in 10 mL of distilled water. It was given to the animals orally by gastric tube at a single daily dose of 29 mg/kg body weight.

Soybean: water soluble soybean fiber (WSSF) was prepared in Department of Nutrition in the National Research Center. It was prepared from defatted soybean, its molecular weight is 50000. it was added in a dose of (50 gm/kg of diet) to the standard diet (*Maksimovic et al., 2005*).

Activated protein C: a natural anticoagulant was obtained from Eli-Lilly Company. Each 1 mg was dissolved in 1 ml isotonic sodium chloride solution. It was injected to the animals interaperitoneal (I.P.) at a single daily dose of 5 mg/kg body weight (*Leeder et al., 1994*).

Animals groups:

The present study was carried out on 30 adult male albino rats weighing 180-200 grams each. All animals were kept under standard laboratory conditions with free access to food and water throughout the study period. They were kept for one week for acclimatization before the experiments in clean properly ventilated cages. The animals were divided into four groups:

Group I (Control group): It was further subdivided into 3 subgroups:

- a. Subgroup **I(a)**: Included 5 animals that received no treatment.
 - b. Subgroup **I(b)**: Included 5 animals that received (WSSF) as the previously mentioned doses, route of administration, daily for 6 weeks.
 - c. Subgroup **I(c)**: Included 5 animals that were injected I.P. at single daily dose by activated protein C 5 mg/kg for 6 weeks.
- **Group II:** Included 5 rats which were received amiodarone at a single daily dose of 29 mg/kg body weight orally for 6 weeks.
 - **Group III:** Included 5 rats which received amiodarone and (WSSF) as the previously mentioned doses, route of administration, daily for 6 weeks.
 - **Group IV:** Included 5 rats received amiodarone

and activated protein C as the previously mentioned doses, route of administration, daily for 6 weeks.

At the appropriate time, all animals were sacrificed and thoracotomy was done. The lungs were dissected after intracardiac perfusion and intratracheal injection with 4% paraformaldehyde in 0.1 M phosphate buffered solution (pH 7.4) containing 2.5 glutaraldehyde solution to inflate the lungs. The trachea was ligated just caudal to the larynx and the thoracic contents were removed as one unit, then both lungs were excised.

For light microscopy, the lung specimens were fixed by immersion in 10% buffered formalin solution for 24 hours, dehydrated in a graded ethanol series, cleared in xylene and then embedded in paraffin wax. Sections (5µm thick) were stained with haematoxylin and eosin (H and E), with Mallory's trichrome stain for demonstration of collagen fibres (*Fraire et al., 1993*).

For Immunohistochemistry, paraffin sections of the lung specimens were deparaffinized, hydrated, washed, heated in buffer citrate and incubated for 30 minutes with rabbit serum. Then the slides from each group were incubated with anti-plasminogen activator inhibitor-1 (PAI-1) mouse monoclonal antibodies (Catalogue Numbers 3785, American Diagnostica, Stamford, CT) at a 1:200 dilution for 22 hours at room temperature. On the next day, all slides were washed in buffered phosphate solution, incubated with biotinylated anti-mouse antibody dilution 1:200 for 1 h (Vector Laboratories, Burlingame, Calif., USA). Then, they were incubated in avidin-biotin-peroxidase complex (Patts, Glostrup, Denmark) chromogen for few minutes. Finally all lung sections were counterstained with Mayer's haematoxylin catalogue number (TA-060-MH). The specificity of the immune reactions was tested by replacing the primary antiserum with phosphate buffer saline as a negative control (*Jessurun et al., 1998*).

For electron microscopy, thin slices of the lungs were fixed in 2.5% phosphate buffered glutaraldehyde solution (pH7.4) for 2 hours and postfixed in 1% osmium tetroxide solution in phosphate buffer for 2 hours. Subsequently, the specimens were dehydrated in a graded series of ethanol, treated with propylene oxide and embedded in Epon. After heat polymerization the sections were cut using an ultramicrotome. Ultrathin sections were double-stained with uranyl acetate and lead citrate to be examined by a JEOL transmission electron microscope (JEM 1010, Japan), at 80 KV in the Faculty of Science, Ain Shams University.

Morphometric Study:

The morphometric data were obtained using Leica Qwin 500 UK, image analyzer computer system in Histology Department, Faculty of Medicine Cairo University. The image analyzer was first calibrated automatically to convert the measurement units (pixels) produced by the image analyzer program into actual micrometer units.

Using the interactive measuring menu the thickness of the interalveolar septa were measured in haematoxylin and eosin-stained sections at a magnification of 400. In each section ten readings were obtained from ten randomly-chosen non-overlapping fields and the mean values and standard deviations were calculated automatically by the image analyzer. Using the measuring field menu and by the color detecting method the area % of positive plasminogen activator inhibitor-1 immunostained area as well as the collagen fibers were measured in plasminogen activator inhibitor-1 immunostained and Mallory's trichrome stained sections. The measurements were done at a magnification of 400. Ten readings from ten randomly-chosen non-overlapping fields were obtained. The thickness of the interalveolar septa and the area % of + ve plasminogen activator inhibitor-1 Immunostained area as well as collagen fibers, all data were expressed as mean (X), \pm standard deviation (SD) and student's test was used to compared between different groups. P-value was calculated using Minitab program and $P < 0.05$ was considered non-significant while $P < 0.001$ was highly significant.

3. Results:

I- Light Microscopic Results:

Examination of sections stained with H and E from the control animals (Group I) revealed that all subgroups showed normal histological structure of the lung. The interalveolar septa were seen to be thin and the alveoli and alveolar sacs appeared clear and patent (fig. 1).

Mallory's trichrome-stained sections showed fine collagen fibers around the bronchioles and to a lesser extent in the interalveolar septa (fig. 2). Moreover, PAI-1 immunoreactivity of lung sections of control group revealed negative immune reaction to PAI-1 almost in all fields (fig. 3).

As regards amiodarone-treated animals (group II), in Hx. and E.- stained sections, the changes were variable among the animals. Complete loss of normal lung architecture was observed with loss of continuity of alveolar epithelium (figs. 4, 5, 6).

Meanwhile, there was extensive thickening and distortion of the interalveolar septa with dilatation and congestion of the pulmonary blood vessels (figs.

4,5). Focal areas of overexpansion, areas of attenuated intrapulmonary air passage and alveolar lining epithelium with destroyed inter-alveolar septa were observed (figs. 5, 7).

Homogeneous eosinophilic material with perivascular and peribronchial cellular infiltration and in the interstitial tissue were observed with vacuolated macrophages inbetween them (figs. 4, 5, 6, 7, 8).

Injury of the lining epithelium of some alveoli and bronchioles was observed with sloughing of some cellular debris and some pneumocytes type II appeared vacuolated with dark nuclei (figs. 6,7, 8).

Mallory's trichrome staining showed an apparent increase in the content of collagen fibers in the perivascular area and in the thickened inter-alveolar septa (fig. 9). Perivascular and peribronchial deposition of coarse collagen fibers was observed (fig.10). Regarding PAI-1 immunoreactivity, sections revealed strong immunopositivity for PAI-1 and a statistically highly significant increase in the area % of the reaction appeared as brownish cytoplasm (figs. 11,12,13).

Examination of sections stained with Hx. and E from amiodarone and soybean-treated animals (group III) showed decrease in the interalveolar thickness while some areas with thickened septa were observed (fig. 14). Moreover, animals treated with amiodarone and activated protein C (group IV) showed preservation of normal architecture, nearly similar to the control group (fig. 15).

However, the increase in collagen fibers was still observed in group III (fig. 16), but group IV was appeared similar to the control group in (fig. 17).

On the other hand, the lung section of group III showed moderate decrease in the area % of the immune reaction to PAI-1 (fig. 18). However, negative to moderate immune reaction to PAI-1 in the area % was observed in group IV (fig. 19).

II- Electron microscopic results:

Ultrastructural examination showed the two types of pneumocytes lining the alveoli. Type I pneumocytes, were flattened in shape with a flat large nucleus and smooth surface. Type II pneumocyte were cuboidal and had central nuclei with few short scattered microvilli on their cell surfaces. Type II pneumocytes were characterized by the presence of many electron-dense concentric lamellae of secretory materials (fig. 20).

In amiodarone-treated animals (group II), type II pneumocyte showed degenerative changes of its lamellar bodies, nearly devoid of its lamellation and numerous cytoplasmic vacuoles and dense bodies (figs. 21, 22, 23, 24). The interstitium showed extravasations of RBCs, many mononuclear cellular infiltration and transversely oriented collagen fibers (figs. 22, 23, 24).

Thickening of the inter-alveolar septa and alveolar macrophage were observed with vacuolated cytoplasm and lamellar inclusions (figs. 22, 25). Examination of group III showed improved picture as compared to group II as some lamellar bodies in type II pneumocyte filled with parallel lamella (fig. 27). Sections of group IV revealed that, most of the observed changes in group II were decreased in both severity and frequency. Type II pneumocytes appeared nearly similar to the control (fig. 28).

Morphometric and statistical analysis showed non-significant changes ($P>0.05$) in the means of inter-alveolar thickness in subgroups Ib and Ic and a high significant increase ($P<0.001$) in group II as compared with subgroup Ia. Regarding group III and IV there was a decrease in the thickening of the interalveolar septa as compared to group II but there was a non-significant change ($P>0.05$) as compared with subgroup Ia (Table 1).

Table (1): The mean thickness of the interalveolar septa in different groups as compared to the control subgroup I-a by student's t-test.

| Group | Mean \pm S.D. | T-value | P-Value | Significance |
|-------|------------------|---------|---------|--------------|
| I-a | 1.83 \pm 0.35 | | | |
| I-b | 1.84 \pm 0.42 | 0.03 | >0.05 | N.S. |
| I-c | 2.10 \pm 0.39 | 0.98 | >0.05 | N.S. |
| II | 19.01 \pm 5.11 | 7.01 | <0.001 | H.S. |
| III | 2.60 \pm 0.41 | 1.91 | >0.05 | N.S. |
| IV | 1.98 \pm 0.52 | 1.96 | >0.05 | N.S. |

There was a non-significant change ($P>0.05$) in the mean area of percentage of collagen in subgroups Ib and Ic as compared to subgroup Ia. There was a highly significant increase (<0.001) in mean area of percentage of collagen content in animals of group II

as compared to the control subgroup Ia. Regarding group III and IV there was a non-significant change ($P>0.05$) in the mean area of percentage of collagen as compared to the control group Ia (Table 2).

Table (2): Mean area percentage of collagen content/field in different groups compared to the control subgroup Ia by student's t-test.

| Group | Mean \pm S.D. | T-value | P-Value | Significance |
|-------|-----------------|---------|---------|--------------|
| I-a | 4.11 \pm 1.01 | - | | |
| I-b | 4.13 \pm 0.52 | 0.27 | >0.05 | N.S. |
| I-c | 4.25 \pm 0.31 | 0.44 | >0.05 | N.S. |
| II | 37.5 \pm 4.11 | 8.10 | <0.001 | H.S. |
| III | 8.15 \pm 2.16 | 6.06 | >0.05 | N.S. |
| IV | 8.12 \pm 2.13 | 6.03 | >0.05 | N.S. |

As regards the means of area percentage of PAI-1/field, there was a non-significant change in subgroups Ib and Ic, as compared to the control subgroup Ia ($P > 0.05$), a highly significant increase

(<0.001) in the means of area % of PAI-1/field in animal of group II and a non-significant increase (>0.05) in animals of groups III and IV as compared with the control subgroup Ia (Table 3).

Table (3): Mean area percentage of PAI-1/field in different groups compared to the control subgroup I-a by student's t-test.

| Group | Mean \pm S.D. | T-value | P-Value | Significance |
|-------|------------------|---------|---------|--------------|
| I-a | 8.19 \pm 3.01 | - | | |
| I-b | 8.56 \pm 1.97 | 0.32 | >0.05 | N.S. |
| I-c | 8.01 \pm 2.04 | 0.04 | >0.05 | N.S. |
| II | 27.22 \pm 3.96 | 8.99 | <0.001 | H.S. |
| III | 14.85 \pm 8.72 | 3.11 | >0.05 | N.S. |
| IV | 14.81 \pm 8.53 | 3.15 | >0.05 | N.S. |

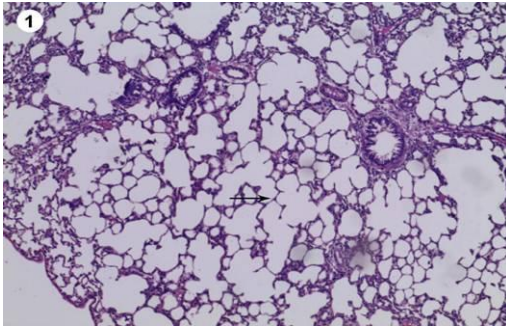


Fig. 1: A photomicrograph of rat lung of the control group (Group I) showing normal lung architecture with thin inter-alveolar septa (arrow). Notice the normal clear alveoli and alveolar sacs. Hx. & E.; X 200

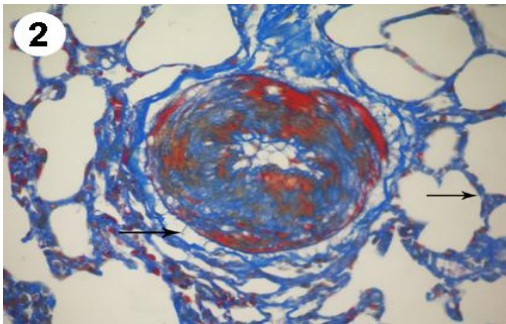


Fig. 2: A photomicrograph of rat lung of the control group (Group I) showing few scanty delicate collagen fibers in the inter-alveolar septa and surrounding the bronchioles (arrow). Mallory's trichrome; x 400

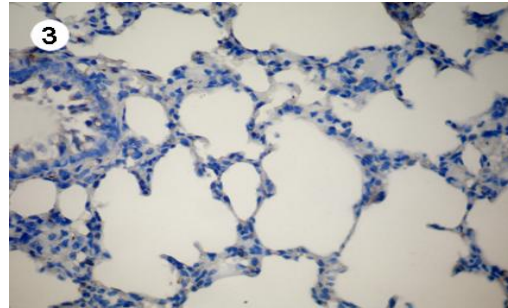


Fig. 3: A photomicrograph of rat lung of the control group (Group I) showing negative immune reaction to plasminogen activate inhibitor-1 (PAI-1) in the inter-alveolar septa, alveolar cells, peribronchial areas and bronchial epithelium. Immunostaining & Hx. counterstain.;x 400

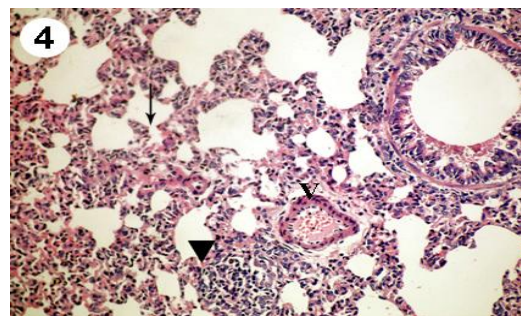


Fig. 4: A photomicrograph of rat lung from amiodarone-treated group (Group II) showing thickened inter-alveolar septa, loss of continuity of alveolar epithelium (arrow), congestion and dilatation of the pulmonary blood vessels (V) with perivascular and interstitial mononuclear cellular infiltration in the form of nodules (arrow head). Hx. & E.; x 200

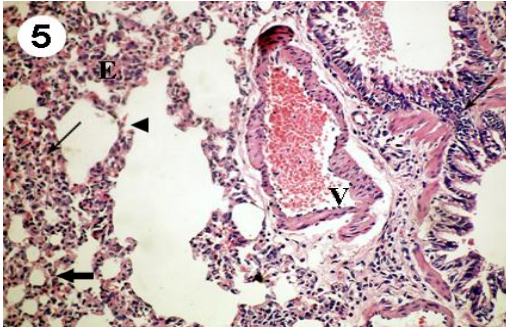


Fig. 5: A photomicrograph of rat lung from amiodarone-treated group (Group II) showing a congested blood vessel (V), interstitial and peribronchiolar mononuclear cellular infiltration (thin arrow), with focal areas of overexpansion with destroyed interalveolar septa (head arrow). Notice the presence of eosinophilic material in thickened interalveolar septa (E) and the collapsed alveolar spaces (thick arrow). Hx. & E.; x 200

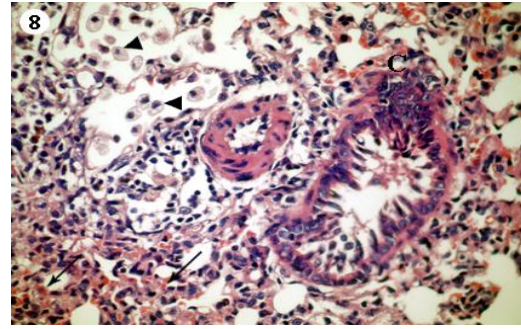


Fig. 8: A photomicrograph of rat lung from amiodarone-treated group (Group II) showing, loss of normal architecture and subepithelial cellular infiltrate encroaches on the bronchiolar lumen (C), sloughing of vacuolated pneumocytes type II with dark pyknotic nuclei inside alveoli (arrow head) and extravasation of blood in alveolar spaces with marked collapse of many alveoli (arrow). Hx. & E.; x 400

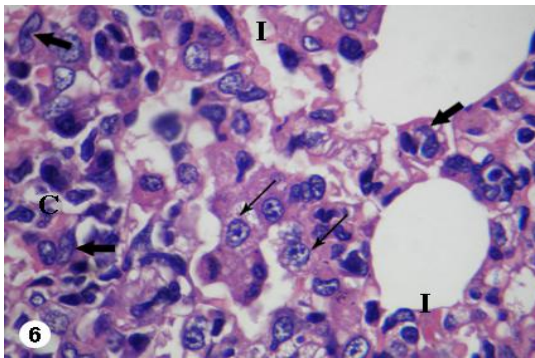


Fig. 6: A photomicrograph of rat lung from amiodarone-treated group (Group II) showing apparent increase in both size and number of type II pneumocytes with highly vacuolation of their cytoplasm (thin arrow). Notice homogenous eosinophilic material in the interstitial tissue (I), cellular infiltration (C) and macrophages in between them (thick arrow). Hx. & E.; x 1000

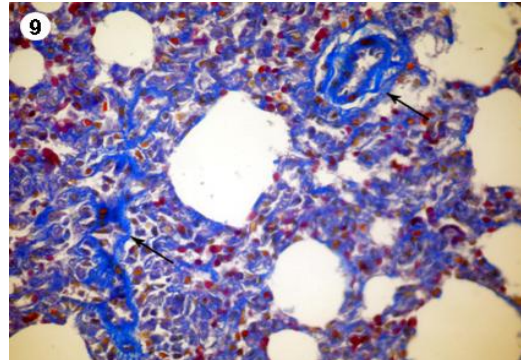


Fig. 9: A photomicrograph of rat lung from amiodarone-treated group (Group II) showing increase in the collagen fibers perivascular and in the thickened inter-alveolar septa (arrow). Mallory's trichrome; x 400

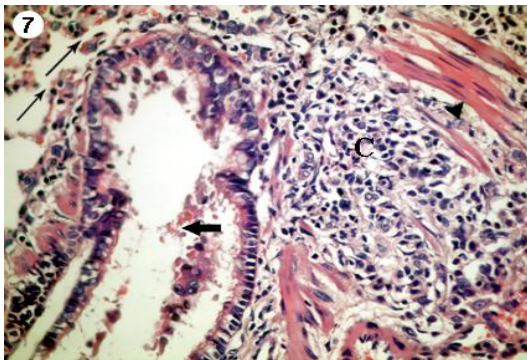


Fig. 7: A photomicrograph of rat lung from amiodarone-treated group (Group II) showing loss of lung architecture with extensive infiltration by mononuclear inflammatory cells (C), areas of destroyed inter-alveolar septa (thin arrow) and areas of bundles of collagenous fibres in inter-alveolar septum (arrow head). Sloughing of bronchiolar lining epithelium (thick arrow) were also noticed. Hx. & E.; x 400

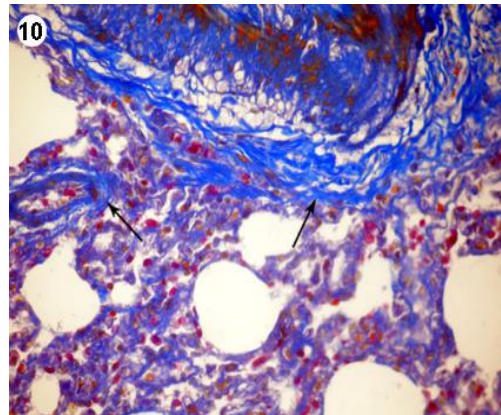


Fig. 10: A photomicrograph of rat lung from amiodarone-treated group (Group II) showing coarse collagen deposition (arrow) in perivascular and in peribronchiolar areas. Mallory's trichrome; x 400

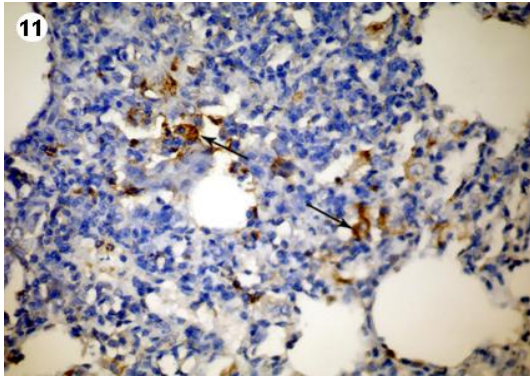


Fig. 11: A photomicrograph of rat lung from group II showing positive immune reaction to PAI-1 in some alveolar cells and thick inter-alveolar septa (arrow). Immunostaining & Hx. counterstain.;x 400

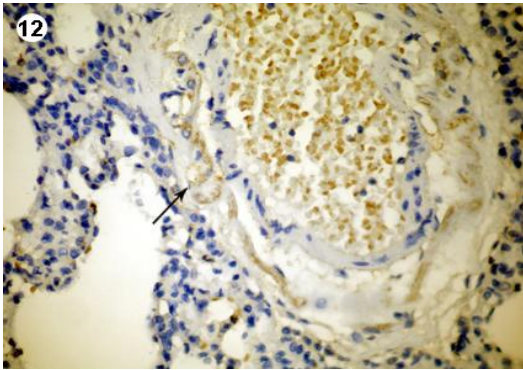


Fig. 12: A photomicrograph of rat lung from group II showing positive immune reaction to PAI-1 in the perivascular area (arrow). Immunostaining & Hx. counterstain.;x 400

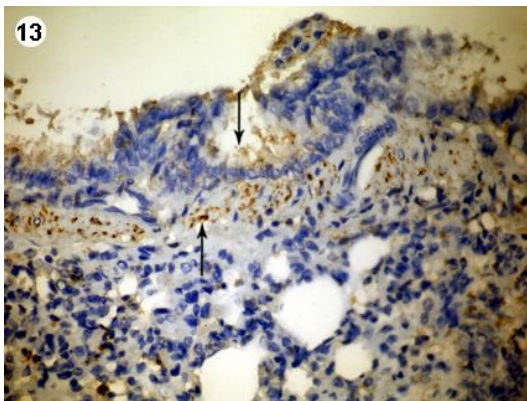


Fig. 13: A photomicrograph of rat lung from group II showing positive immune reaction to PAI-1 in the peribronchiolar areas and bronchiolar epithelium (arrow). Immunostaining & Hx. counterstain.;x 400

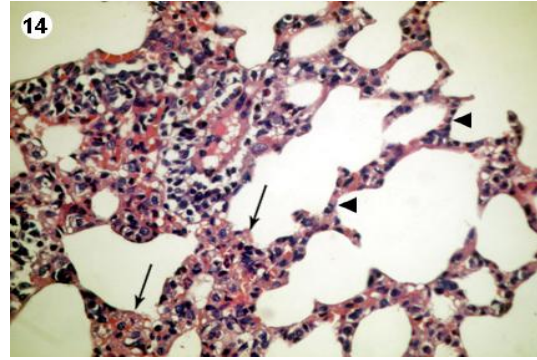


Fig. 14: A photomicrograph of rat lung from amiodarone and soybean treated group (Group III) showing decrease in the inter-alveolar thickness (arrow head). Some areas with thickened septa were observed (arrow). Hx. & E.; x 400

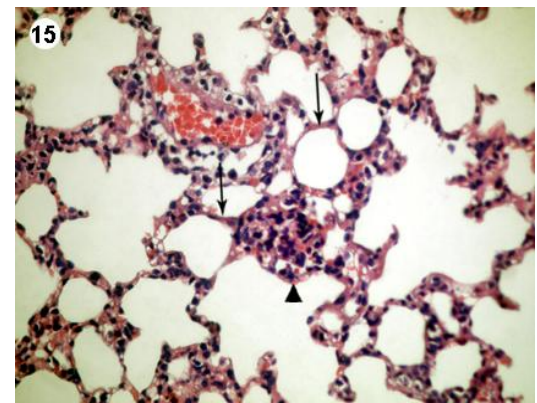


Fig. 15: A photomicrograph of rat lung from amiodarone and activated protein C-treated group (Group IV) showing preserved normal architecture with decrease in the inter-alveolar thickness to be more or less as control group (arrows) but with few thickened infiltrated parts (arrow heads). Hx. & E.; x 400

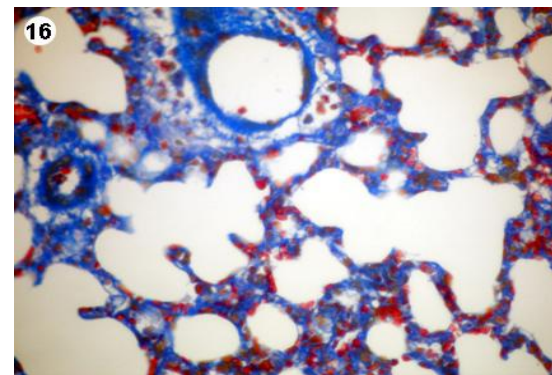


Fig. 16: A photomicrograph of rat lung from group III showing decrease in the collagen fibers in the inter-alveolar septa and in the peribronchiolar areas. Mallory's trichrome; x 400

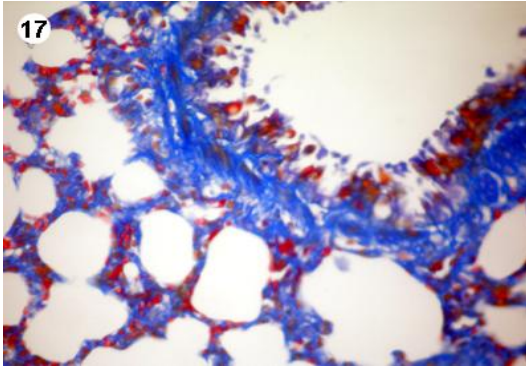


Fig. 17: A photomicrograph of rat lung from group IV showing decrease in the collagen fibers in the thin interalveolar septa and peribronchiolar areas to be more or less similar to control group. Mallory's trichrome; x 400

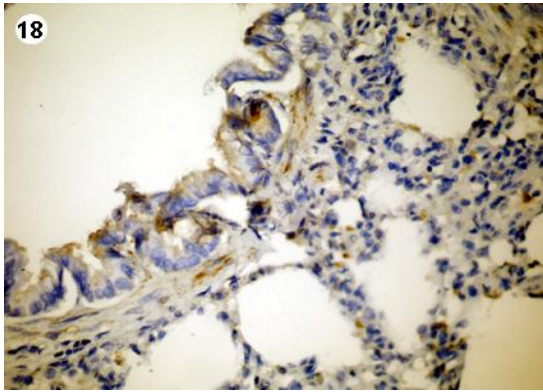


Fig. 18: A photomicrograph of rat lung from group III showing moderate immune reaction to PAI-1 in the interalveolar septa, peribronchiolar area and in bronchiolar epithelium. Immunostaining & Hx. counterstain.;x 400

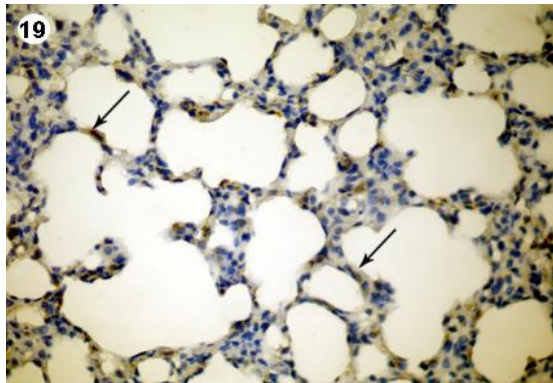


Fig. 19: A photomicrograph of rat lung from group IV showing negative to moderate immune reaction to PAI-1 in most alveolar cell walls and in the inter-alveolar septa (arrows). Immunostaining & Hx. counterstain.;x 400



Fig. 20: An electron micrograph of rat lung from control group showing type I pneumocyte containing flat nucleus (N) and type II pneumocyte with many electron dense concentric lamellae of secretory material (thin arrow) and central nucleus with euchromatin (arrow head) Notice the microvilli on the surface of type II pneumocyte (thick arrow).

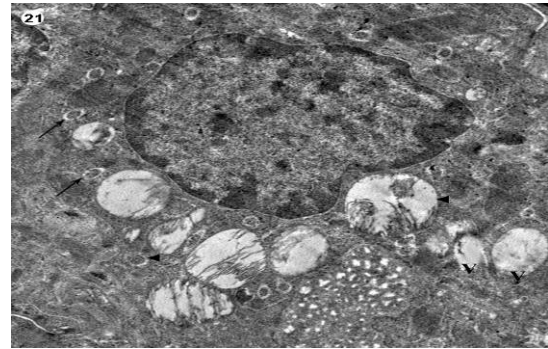


Fig. 21: An electron micrograph of rat lung from group II showing type II pneumocyte with degenerative changes of its lamellar bodies (arrow head), many cytoplasmic vacuoles (V) and numerous dense bodies (arrow). Notice absence of microvilli. X 3,000

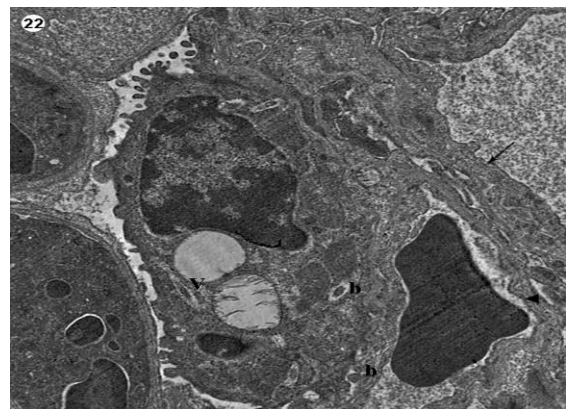


Fig. 22: An electron micrograph of rat lung from group II showing type II pneumocyte with numerous cytoplasmic dense bodies (b) and vacuoles (V), thickening of interalveolar septa (arrow) with congested blood vessels (arrow head). x 2,500

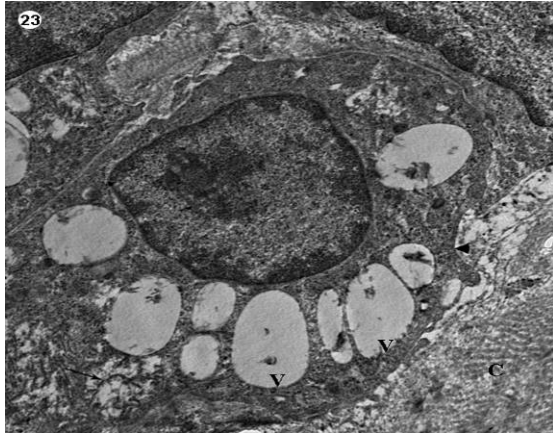


Fig. 23: An electron micrograph of rat lung from group II showing type II pneumocyte nearly devoid of the secretory material in its lamellar bodies with presence of many large vacuoles (V), rarefaction of the cytoplasm (arrow) and absence of microvilli (arrow head). Notice transversely oriented collagen fibers (C). x 3,000

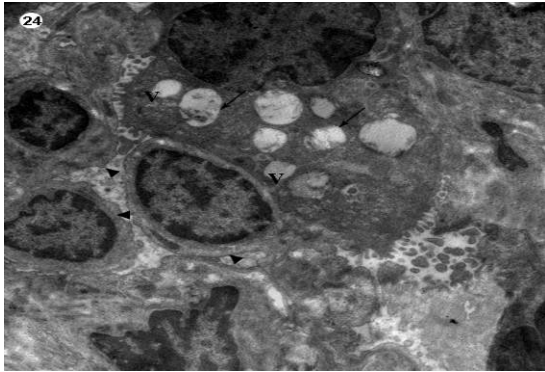


Fig. 24: An electron micrograph of rat lung from group II showing type II pneumocyte with vacuolated cytoplasm (V) and numerous disorganized lamellar bodies (arrow) that lose their lamellar appearance. Notice many mononuclear cellular infiltration (arrow head). x 2,000



Fig. 25: An electron micrograph of rat lung from group II showing an alveolar macrophage with its eccentric kidney shaped nucleus (N), irregular outlines and vacuolated cytoplasm (V) with occasional lamellar inclusions (thin arrow) and lysosomes (L). Notice, marked thickening of inter-alveolar septa (thick arrow). x 3,000

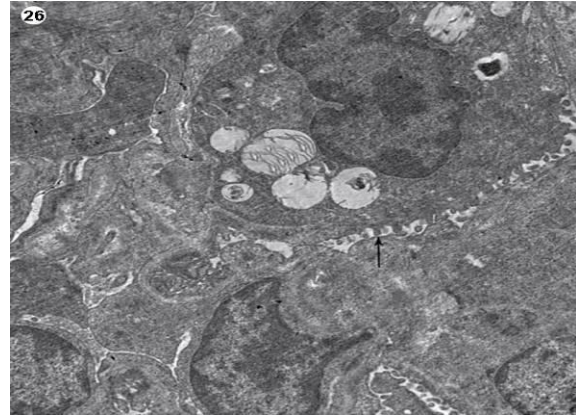


Fig. 26: An electron micrograph of rat lung from group III showing type II pneumocyte with many lamellar bodies, some of them filled with parallel lamella. Notice microvilli (arrow). x 2,500

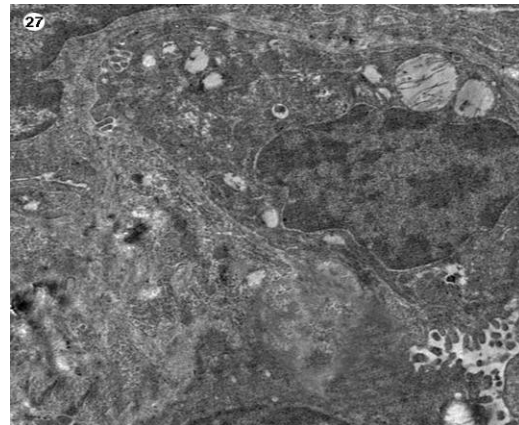


Fig. 27: An electron micrograph of rat lung from group IV showing type II pneumocyte has decreased number of lamellar bodies with normal parallel lamella, rounded central nucleus with euchromatin and has microvilli. x 3,000

4. Discussion:

The antiarrhythmic drug amiodarone produces lung toxicity in humans and animals. Some data suggested a role for oxidative stress in amiodarone-induced lung toxicity. Amiodarone inhibits mitochondrial complex I and II respiration and produces mitochondrial dysfunction in lung epithelial cells and macrophages. Also, amiodarone increases the levels of reactive oxygen species (ROS) and oxidized glutathione. Further studies have revealed that amiodarone is metabolized to an early radical that may give rise to other ROS (Massey *et al.*, 1995). Both catalytic and scavenger antioxidants have been shown to attenuate amiodarone-induced lung injury. In addition, phenolic antioxidants were effective in limiting amiodarone-induced ROS and lung injury. The resemblance of the morphological changes in amiodarone-treated rats lungs to pulmonary injury in

humans suggests that this form of chemical injury may serve as useful model of this disease entity (Esmon *et al.*, 1997).

The etiology of amiodarone pulmonary toxicity is unknown. However, several causes have been proposed including direct toxicity, the involvement of hypersensitivity, elevated oxidant involvement and drug-induced alterations in membrane properties. It has been postulated that the cause is complex and multifactorial, possibly involving several of these mechanisms (Shimizu *et al.*, 2003).

Several mechanisms have been postulated to explain the suppressive effect of APC on lung injury. One mechanism is the ability of APC to suppress inflammation. The anti-inflammatory activity of APC is a reflection of its ability to suppress the secretion of inflammatory cytokines, such as TNF- α and monocyte chemoattractant protein-1 from the inflammatory cells and to inhibit the activation and extravasation of leukocytes. APC also may inhibit the lung injury by binding to and inhibiting plasminogen activator inhibitor-1 leading to increased activity, of plasminogen activator and a net enhancement of fibrinolytic function (Vangerow *et al.*, 2007). APC, as anticoagulant activity block interalveolar fibrin deposition and thrombin generation. APC is able to activate pro-matrix metalloproteinases and in that way suppresses the deposition of extracellular matrix in the lung (Jian *et al.*, 2005).

A further antifibrotic activity of APC is its ability to inhibit the expression of platelet-derived growth factor (PDGF) on macrophages, bronchial epithelial cells and pulmonary artery endothelial cells. PDGF is a potent mitogenic factor for fibroblasts. Moreover, inhibition of PDGF secretion by APC blocks the development of lung injury (Emmons and Peterson, 2001).

Previous studies mentioned that, soybean water soluble fiber ameliorated the lung toxicity changes induced by amiodarone and attributed this effect to its compounds. These compounds include a protease inhibitor, trypsin inhibitor, isoflavones (genistein and diadzein), saponins, inositol (hexaphosphate phytic acid) and sitosterol (Emmons and Peterson, 2001). Polyphenols compounds are often chain-breaking antioxidants and some have been used in the food industry as preservative. In general, they require larger doses or concentrations to produce antioxidant effects in model system because their lower rates of reaction with ROS and their limited ability to be recycled endogenously. Also, another study found positive correlation between the content of total isoflavone and genistein with antioxidant capacity (Silva *et al.*, 2002).

A recent study showed that isoflavones might have their effects on the pathways by inducing the

gene expression or modifying the enzyme activity rather than acting directly as free radical scavenger. On the other hand, other researchers found that all tested soybean isoflavones and glycosides appeared to be much weaker antioxidants than green tea and α -tocopherol (Bolt *et al.*, 2001). Other research works showed that the active components of soy products responsible for these effects rather than isoflavones including phospholipids, lecithin, low but considerable content of linolenic acid (7.8%) and α -tocopherol (Card *et al.*, 2003).

The amiodarone induced pulmonary toxicity manifested by many criteria included a mixed cellular exudates in the interstitium, protein exudates in air spaces with or without leukocytes, proliferation of lining epithelium, gradual progression to fibrosis, continuing evidence of cellular reaction and diffuse distribution (Massey *et al.*, 1995). The present work showed that amiodarone could induce pulmonary injury in the form of hyperplasia of type II pneumocytes, large foamy macrophages with mononuclear cellular infiltrations in lung parenchyma and thickened interalveolar septa. These coincide with other workers who observed amiodarone pneumotoxicity after 4 weeks of therapeutic dosage manifested by congested blood capillaries with perivascular cellular infiltration (Dhainaut *et al.*, 2004).

The current experiment revealed a remarkable mononuclear cellular infiltration peribronchiolar, perivascular and in the interstitial tissue. Hypersensitivity and immunological reactions could be important in the pathogenesis of amiodarone-induced interstitial pneumonitis, where injured epithelial lung cells release increased amounts of inflammatory cytokines in response to amiodarone (Jian *et al.*, 2005). These cytokines initiate the inflammatory reaction and attract inflammatory cells that were observed in the current study. The presence of red blood corpuscles in the extravascular tissue can also initiate the inflammatory reaction and attract the infiltrating cells to the site of congestion.

The present study showed many areas of destruction of the interalveolar septa and connection of many alveoli together with formation of large irregular air spaces. These morphological changes are compatible with emphysematous lung and similar findings described by other researchers (Looney *et al.*, 2009). Fragmentation of the alveolar septa could be due to proteolytic destruction of the lung parenchyma by the proteolytic enzymes released from the inflammatory cells. Moreover, in the present study dark pyknotic nuclei indicated the occurrence of apoptosis of alveolar wall or endothelial cells and is sufficient to cause pulmonary emphysema, even without the accumulation of inflammatory cells.

Disruption of the balance between apoptosis and replenishment of structural cells in the lung might contribute to the destruction of lung tissue leading to emphysema (Esmon *et al.*, 1997). Areas of collapsed alveoli and thickened interalveolar septa which were observed in our study were present side by side with the emphysematous ones. These alterations could be attributed to combined endothelial and epithelial injury that leads to basement membrane denudation, resulting in collapse of alveolar septa.

Congested blood vessels in our study was explained to be due to direct vasodilator effects of amiodarone by blocking alpha receptors and calcium channels inhibitory effects. EM study of capillary endothelial cells appeared swollen with vacuolization in their cytoplasm. This is explained by earlier study as amiodarone increased production of free oxygen radicals and capillary permeability. The capillary endothelial cells showed cellular swelling and detachment from underlying basement membrane, vascular congestion and thickening of the wall of arterioles were also reported (Oyama *et al.*, 2005).

The morphometric study in the present work revealed a highly significant increase in the thickness of the interalveolar septa in amiodaron-treated rats as compared with the control ones. This might be due to cellular infiltration in the septa and increased collagen content. This coincides with a previous study that showed hypercellularity and edema of interalveolar septa in amiodarone-treated group (Pitsiavas *et al.*, 1997). The original hypothesis for the pathogenesis of pulmonary fibrosis is that chronic inflammation stimulates the ability of fibroblasts to migrate, proliferate, and produce the extracellular matrix, thereby resulting in parenchymal fibrosis. A new hypothesis for the pathogenesis of pulmonary fibrosis suggesting that the inappropriate regeneration of the sequentially injured epithelium is sufficient to stimulate fibroblasts, resulting in irreversible parenchymal fibrosis (Taylor *et al.*, 2003).

As regards to type II pneumocytes, the current work also showed a highly significant increase in number of type II pneumocytes and an apparent increase in their size denoting cellular hyperplasia and hypertrophy suggesting that the type II cells are attempting to proliferate to regenerate the injured epithelium, particularly if there is destruction of the sensitive type I pneumocytes. Similar changes of the epithelial lining were previously reported by many researchers. Proliferation of type II pneumocytes was shown to be the most sensitive pathological indicator of alveolitis. Moreover, the density of type II pneumocytes could be a useful index for evaluating alveolar damage even in mild alveolitis. As regards to EM examination, type II pneumocytes showed degenerative changes of lamellar bodies in their

cytoplasm in amiodarone experimental group. This observation is in agreement with a previous work which explained that these lamellar bodies were the source of pulmonary surfactant (Yasuda *et al.*, 1996).

Some cells contain numerous dense bodies. Our present work is also in agreement with a previous research that suggested that dense bodies were due to a secondary lipid storage disorders induced by amiodarone. On the other hand, an earlier report found that chronic amiodarone therapy inhibited lysosomal phospholipases leading to phospholipids accumulation that appeared as dense bodies (Sunderji *et al.*, 2000).

In group II, the macrophages showed with lamellar bodies and pale vacuolated cytoplasm. This is in agreement with another study that suggested the increase in number was due to increased production of surfactant by type II pneumocytes (Sunderji *et al.*, 2000). As regards to the vacuolated, foamy appearance of macrophages, earlier research attributed it to secondary phospholipidosis caused by amiodarone. Another study explained that the cause for these inclusions in the macrophages was due to ingestion of surfactant and foreign particles as the macrophages played an important role in the lung defense (Lafuente-Lafuente *et al.*, 2009). They added that amiodarone inhibited phospholipase enzyme of lysosomes leading to the increase of phospholipids in lysosomes and appearance of lamellar bodies in macrophagy.

The collagen fibers content of the interalveolar septa was increased. This finding is attributed to immune and inflammatory mechanisms that leads to fibroblast stimulation and collagen deposition (Massey *et al.*, 1995). The increased amount of lung collagen detected in the experimental rats and its deposition in an abnormal locations indicated occurrence of interstitial fibrosis. This fibrosis was reported by an earlier work to be the end result of alveolar damage which may occur as a sudden acute incident or as a slowly developing process (Wang *et al.*, 1992). After concomitant use of APC, there was a decrease of collagen fiber content. This is in agreement with previous report who stated that APC was able to attenuate lung injury in rats. The density of neutrophil increased significantly with segmented nuclei and highly condensed chromatin in the lung interstitium (alveolar spaces). Also, eosinophils with bilobed nuclei could be observed in the alveolar wall and dilatation of rough endoplasmic reticulum that was attributed to disruption of protein sorting pathway (Nicolescu *et al.*, 2007).

Previous studies indicate that activation of the coagulation cascade may play an important role in the pathogenesis of lung injury (Jian *et al.*, 2005). In the present experiments, we examined the effect of APC

and soybean on amiodarone-induced lung toxicity. Histological examination showed that both agents alleviated inflammatory cell infiltration and progression of lung inflammation. The pulmonary reaction following the administration of intraproteineal amiodarone in the experimental animals has been extensively used the pathogenesis of the inflammation is the subject of further investigation. In the present study we found that dietary supplementation with soybean was effective in decreasing pulmonary toxicity induced by AM in vivo. The histological picture of lungs of rats given the soybean-enriched diet was near the control values at 36 days following AM administration. The soybean-enriched diet with APC decreased the AM-induced damage to the lung so that their appearance was similar to the control.

Corresponding author

Maha Mohamed Abo Gazia

Histology Department, Faculty of Medicine, Al-Fayoum University

mahaabogazia@yahoo.com

References:

Blake, T.L. and Reasor, M.J. 1995. Pulmonary responses to amiodarone in hamsters: Comparison of intratracheal and oral administrations. *Toxicology and Applied Pharmacology* . 131, 325–331.

Bolt, M.W., Racz, W.J., Brien, J.F. et al., 2001. Effects of vitamin e on cytotoxicity of amiodarone and n- desethylamiodarone in isolated hamster lung cells. *Toxicology* 166: 109-118.

Card, J.W., Racz, W.J., Brien, J.F., et al., 2003. Differential effects of pirfenidone on acute pulmonary injury and ensuing fibrosis in the hamster model of amiodarone-induced pulmonary toxicity. *Toxicological Sciences*. 75: 169-180.

Chambers, R.C., 2008. Procoagulant signaling mechanisms in lung inflammation and fibrosis: novel opportunities for pharmacological intervention? *British Journal of Pharmacology* 153:367-378.

Dhainaut, J.F., Yan, S.B., Claessens, Y.E. 2004. Protein C/activated protein C pathway: overview of clinical trial results in severe sepsis. *Critical Care Medicine* 32: 194-201.

Emmons, C.L., and Peterson, D.M. 2001. Antioxidant activity and phenolic content of oat as affected by cultivar and location. *Crop Science* . 41: 1676–1681.

Esmon, C.T., Fukudome, K., Mather, T., et al., 1997. Inflammation: the protein C pathway. *Fibrinolysis and Proteolysis* 11:143–148.

Fraire, A.E., Guntupalli, K.K., Greenberg, S.D., et al., 1993. Amiodarone pulmonary toxicity: a multidisciplinary review of current status. *Southern Medical Journal* 86(1): 67-77.

Idell, S. 2003. Coagulation, fibrinolysis, and fibrin deposition in acute lung injury. *Critical Care Medicine*. 31: 213–220.

Ishimi, Y., Miyaura, C., Ohmura, M., et al., 1999. Selective effects of genistein, a soybean isoflavone, on Blymphopoiesis and bone loss caused by estrogen deficiency. *Endocrinology* 140: 1893-1900.

Jessurun, G.A., Boersma, W.G. and Crijns, H.J. 1998. Amiodarone-induced pulmonary toxicity. predisposing factors, clinical symptoms and treatment. *Drug Safety* 18: 339-344.

Jian, M.Y., Koizumi, T., Tsushima, K., et al., 2005. Activated protein C attenuates acid-aspiration lung injury in rats. *Pulmonary Pharmacology and Therapeutics* . 18: 291-296.

Lafuente, C., Alvarez, J.C., Leenhardt, A., et al., 2009. Amiodarone concentrations in plasma and fat tissue during chronic treatment and related toxicity. *British Journal of Clinical Pharmacology* . 67: 511-519.

Leeder, R.G., Brien, J.F. and Massey, T.E. 1994. Investigation of the role of oxidative stress in amiodarone-induced pulmonary toxicity in the hamster. *Canadian Journal of Physiology and Pharmacology*. 72(6): 613–621.

Liechtenstein, A.H. 1998. Soy protein, isoflavones and cardiovascular disease risk. *Journal of Nutrition*. 128: 1589-1592.

Looney, M.R., Esmon, C.T., Matthay, M. 2009. The role of coagulation pathways and treatment with activated protein C in hyperoxic lung injury. *Thorax*. 64: 114-120.

Mahwah, N.J. 1996. Effect of dietary genistein on antioxidant enzyme activities in SENCAR mice. *Nutrition and Cancer*. 25: 1-7.

Maksimović, Z., Malenčić, D.J., Kovačević, N. 2005. Polyphenol contents and antioxidant activity of Maydis stigma extracts. *Bioresource Technology* . 96: 873–877.

Malenčić, D., Popović, M., Miladinović, J. 2007. Phenolic content and antioxidant properties of Soybean (*Glycine max* (L.) Merr.) seeds. *Molecules* 12: 576–581.

Martin, W. and Rosenow, E. 1988. Amiodarone pulmonary toxicity: recognition and pathogenesis. *Chest*. 93: 1067-1075.

Massey, T., Leeder, R., Rafeiro, E. et al., 1995. Mechanisms in the pathogenesis of amiodarone induced pulmonary toxicity. *Canadian Journal of Physiology and Pharmacology*. 73(12): 1675-85.

- Messina, M.J.* 1999. Legumes and soybeans: overview of their nutritional profiles and health effects. *The American Journal of Clinical Nutrition*. 70: 439-450.
- Mitchell, J.H., Gardner, P.T., McPhail, D.B., et al.*, 1998. Antioxidant efficacy of phytoestrogens in chemical and biological model systems. *Archives of Biochemistry and Biophysics* . 360: 142-148.
- Nicolescu, A.C., Comeau, J.L., Hill, B.C., et al.*, 2007. Aryl radical involvement in amiodarone-induced pulmonary toxicity: investigation of protection by spin-trapping nitrones. *Toxicology and Applied Pharmacology* . 220: 60-71.
- Oyama, N., Yokoshiki, H., Kamishima, T., et al.*, 2005. Detection of amiodarone-induced pulmonary toxicity in supine and prone positions-high-resolution computed tomography study. *Circulation Journal* 69: 466-470.
- Padmavathy, B., Niranjali, S. and Devaraj, H.* 1992. Lung injury by amiodarone, an antiarrhythmic drug, in male rats. *Indian Journal of Experimental Biology*. 30: 653 – 654.
- Pitsiavas, V., Smerdely, P., Li, M. et al.*, 1997. Amiodarone induces a different pattern of ultrastructural change in the thyroid to iodine excess alone in both BB/W rat and the Wistar rat. *European Journal of Endocrinology*. 137(1): 89-98.
- Richard, J-C., Bregeon, F., Leray, V., et al.*, 2007. Effect of activated protein C on pulmonary blood flow and cytokine production in experimental acute lung injury. *Intensive Care Medicine* DOI 10.1007/s00134-007-0782-0.
- Shimizu, S., Gabazza, E.C., Taguchi, O., et al.*, 2003. Activated protein C inhibits the expression of platelet-derived growth factor in the lung. *American Journal of Respiratory and Critical Care Medicine*, 167:1416-1426.
- Silva, M.M., Santos, M.R., Caroco, G., et al.*, 2002. Structure-antioxidant activity relationships of flavonoids: a re-examination. *Free Radical Research*. 36: 1219-1227.
- Su, S.J., Yeh, T.M., Lei, H.Y., et al.*, 2000. The potential of soybean foods as a chemoprevention approach for human urinary tract cancer. *Clinical Cancer Research*. 6: 230-236.
- Sunderji, R., Kanji, Z. and Gin, K.* 2000. Pulmonary Effects of Low Dose Amiodarone: A Review of the Risks and Recommendations for Surveillance. *Canadian Journal of Cardiology* . 16: pp 1435-1440.
- Taylor, M.D., Antonini, J.M., Roberts, J.R., et al.*, 2003. Intratracheal amiodarone administration to f344 rats directly damages lung airway and parenchymal cells. *Toxicology and Applied Pharmacology* . 188: 92-103.
- Vangerow, B., Shorr, A.F., Wyncoll, D.*, 2007. The protein C pathway: implications for the design of the respond study. *Critical Care*, 11(5): 4.
- Waerhaug, K., Kuzkov, V.V., Kuklin, V.N., et al.*, 2009. Inhaled aerosolised recombinant human activated protein C ameliorates endotoxin-induced lung injury in anaesthetised sheep. *Critical Care* 13:R51.
- Wang, Q., Hollinger, M.A. and Giri, S.N.* 1992. Attenuation of amiodarone-induced lung fibrosis and phospholipidosis in hamsters by taurine and/or niacin treatment. *Journal of Pharmacology and Experimental Therapeutics* 262: 127 – 132.
- Yasuda, S.U., Sausville, E.A., Hutchins, J.B., et al.*, 1996. Amiodarone-induced lymphocyte toxicity and mitochondrial function. *Journal of Cardiovascular Pharmacology* . 28: 94-100.

2/25/12